Effective adsorption of pesticide using biochar derived from *Syzygium Cumini* seeds loaded with lanthanum ferrite nanocomposite, isotherm and kinetics

Anita Kumari[1,2*], Anita Rani[2], Arush Sharma[3]
[1]*Department of Chemistry, School of Basic and Applied Sciences, IEC University, Solan (HP), India.*
[2]*Department of Chemistry, Govt. College Dhaliara, Kangra (HP), India.*
[3]*School of Sciences, Baddi University of Emerging Sciences and Technology (BUEST), Solan, Himachal Pradesh, 173205, India.*
Corresponding Author: Anita Kumari

Abstract: **Chlorpyrifos is the main cause of environmental harm, so creating a sustainable solution is crucial. In the present study *Syzygium cumini* seeds biochar (BR) and *Syzygium cumini* seeds biochar loaded with lanthanum ferrite nanocomposite (BR/LFNC) were explored for the remediation of chlorpyrifos (CS) from water. The nanocomposite was characterized by FESEM and FTIR. Impact of various parameters like temperature, contact time, pH were optimised for the removal of CS. The maximum removal of 80 % and 91% was observed using BR and BR/LFNC at 30 ^{0}C at pH 4.0. Kinetic studies specified the pseudo second order reaction for the removal of CS from water. Adsorption isotherm strongly followed the Langmuir model (R^2 = 0.98).**

Key words: **Adsorption, Biochar; Chlorpyrifos, Isotherm, Nanocomposite**

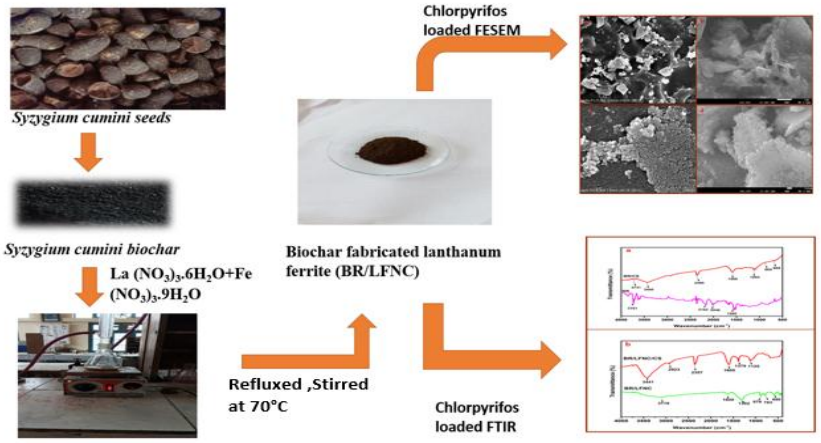

Graphical abstract

INTRODUCTION

The global population is expanding at an accelerated rate, placing tremendous strain on natural resources. The need for food has also increased as a result of the expanding population.

The situation is made worse by the fact that pests damage roughly 40% of agricultural areas [1],[2]. Modern farming methods and a huge number of pesticides are utilized globally to meet the rising demand for agricultural products. By reducing pests, insects, weeds, along with mites that consume crops, pesticides, when used properly, have significantly helped humanity. Chemical fertilisers and weedicides are also used in agricultural areas to increase crop yields.

Chemical spills, washing machines, household use, and industrial effluents are additional sources of pesticides in the environment [3],[4]. Additionally, the dispersed discharge of the drained surplus agrochemicals contaminates the soil and water bodies that receive them. Pesticides are the second-largest chemical found in drinking water [5]. Insecticides or intermediate compounds are known to be nine of the twelve most hazardous chemicals in the world [6] .

The ecology is severely harmed by the excessive and illogical use of pesticides and agrochemicals, which leads to an ecological imbalance that affects humans.

The toxicity of non-target chemicals was the cause of the disease in humans, birds, and aquatic creatures. Pesticides have both acute and long-term impacts, for example neurotoxicity, carcinogenesis, and problems with reproduction. Prolonged exposure to pesticides in human's results in severe illnesses [7].

The majority of insecticides and pesticides used in urban and agricultural contexts contain an active ingredient called chlorpyrifos (CS), an organophosphate compound. Concentrate-emulsions, granules, dusts, wettable powders, and controlled release polymers are some of the several forms of CS that are available [8] . Finding a way to reduce CS levels in the water in which guideline value of drinking water is 2 μg L^{-1} is necessary to asssure the accessibility of safe drinking water [9]. A number of published methods for CS-related aqueous stream decontamination have been proposed, including oxidative degradation [10] , photo-catalytic degradation [11], membrane processes [12] and adsorption approaches [13]-[15]. Given its simplicity of usage and less environmental impact compared to the other techniques, adsorption appears to be a viable technology [16]-[18].

Several water treatment processes utilize carbon-based adsorbents, especially activated carbon which has different levels of adsorption. Activation procedure, pyrolysis temperature, and source material all affect the carbon's properties [19]. Activated carbon in distinct adsorption grades is utilized to remove organic pollutants, heavy metals, dyes, and phenolic compounds [20]-[23].

Natural biomaterials are pyrolyzed at different temperatures to create biochar, a carbon-based sorbent. It has been used in numerous environmental remediation processes, including the removal of pesticides and heavy metals. Green adsorbents, a type of sustainable and renewable adsorbent, are a new trend for heavy metal, pesticide, and antibiotic removal [24]-[29]. Biochar has been used for adsorption as well as the production of ultrafiltration membranes and microbial fuel cells [30]. Adsorbents that utilize natural materials have demonstrated promise in getting rid of CS [31].

The present investigation utilized inexpensive *Syzygium cumini* seed biochar along with its lanthanum ferrite nanocomposite to develop a green nano-sorbent with a high adsorption capacity, recycling capability as well as stability for long term removal of CS from the wastewater.

2. MATERIALS AND METHODS

2.1. Materials

Chlorpyrifos, La $(NO_3)_3.6H_2O$ (Lanthanum nitrate), Fe $(NO_3)_3.9H_2O$ (iron nitrate), NaOH (sodium hydroxide) along with HCl (hydrochloric acid) had been bought from Sigma Aldrich Pvt. Ltd., utilized with no additional purification. DDW (double distilled water) had been employed for employed for producing stock solutions.

2.2. Preparation of biochar

The seeds of *Syzygium cumini* species found in Dharamshala of Himachal Pradesh, India, were used to make biochar (BR). After carefully gathering the seeds, any adhering contaminants were removed by washing them in double distilled water. They were then allowed to dry in the sun for a few days. After drying, the material was screened and woven into uniform-sized particles. For two and a half hours, the produced biomaterial was heated to 600°C in a muffle furnace without oxygen. Every 20 minutes, the temperature rose by 50°C.The material was allowed to cool overnight. The biochar was chemically activated by soaking it in a 1:1 combination of NaOH (5%) and NaClO (6%). After that, mixture was then heated for 30 minutes in a microwave, with temperatures between 60°C and 70°C. After that, the resultant BR was filtered and repeatedly cleaned with DDW until the pH reached a neutral level. Finally, to guarantee thorough drying, the BR was kept for an entire night at temperatures between 50°C and 60°C in an oven. The intended biochar (BR), is ready for additional characterisation and to be use in adsorption investigations.

2.3. Synthesis of biochar fabricated lanthanum ferrite (BR/LFNC)

To synthesis of BR/LFNC, a Single step chemical precipitation technique had been employed. 1M La $(NO_3)_3.6H_2O$ and 4M Fe $(NO_3)_3.9H_2O$ solutions had been prepared utilizing this above method. A magnetic stirrer was employed to continuously stir these solutions as they were mixed in 1:1 ratio. 1 gm BR had been incorporated into metal ion solution with stirring for one hour. Then the solution was treated by adding 15 ml of NaOH (3.0 M) dropwise as well as refluxed for 8hrs utilizing magnetic stirrer at 70 °C temperature. Following centrifugation, for a whole night, precipitates had been dried at 60 °C temperature, while resultant precursor was given the designation BR/LFNC.

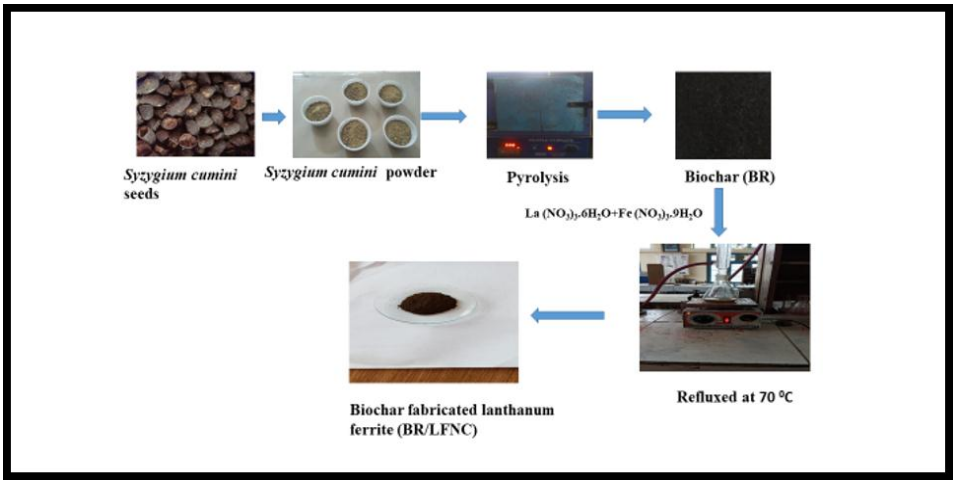

Scheme 1: The Schematic representation of synthesis of the biochar lanthanum ferrite (BR/LFNC) bio-nanocomposite

2.4. Instrumentation

The Hitachi-PU 5.0 kV FESEM had been utilized to examine the surface morphology. A Bruker Optik GmbH 2014 Tensor II machine for FTIR examination in the 4000-400 cm-1 range was employed to analyse the functional groups. FTIR spectra were captured utilizing the KBr technique. This procedure involved vigorously mixing 5-10 mg of material with KBr pellet. With out any moisture, the proper pressure (psi) was applied to form a disk.

2.5. Adsorption experiment

Batch adsorption method was used to observe the ability of BR and BR/LFNC for the adsorption of chlorpyrifos (CS) in aqueous solution. Utilizing 250 mL Erlenmeyer flasks, a fixed quantity of dry adsorbent had been added to 100 mL CS solution in a series of batch tests. The CS solution's Initial concentration varied from 10 - 60 mg/L. For a predetermined amount of time, the mixture was stirred at 120rpm in a rotary shaker. For adsorbent extraction from aqueous phase, flasks had been taken out from shaker as well as centrifuged for 8mins at 6500rpm. Residual concentration of chlorpyrifos had been identified from the filtrate using UV-Visible spectroscopy at 290 nm. The equilibrium study had been executed through by optimizing various parameters for example adsorbent dosage (10-60 mg/L), initial CS concentration (10-60 mg/L, Ph (2.0-12.0), contact time (10-60 min) and temperature.

Equation (1) was applied to determine the removal efficiency Y (%):

$$Y\ (\%) = \frac{C_0 - C_e}{C_o} \times 100 \qquad (1)$$

Where, C_0 and C_e are the initial and is final concentration of CS.

2.6. Kinetics study

Adsorption is a time-dependent process that is important for estimating an adsorbent's effectiveness. Therefore, the following section discusses the applicability of pseudo-first-order and pseudo-second-order:

2.6.1. Pseudo-first-order model

In this model, adsorbate molecule mass transfer from from the aqueous phase to sorption sites is the basis. The expression for this model [32]:

$$\text{Log}\ (q_e - q_r) = \log q_e - \frac{k1}{2.303} t \qquad (2)$$

Here, k_1 specifies the rate constant (h^{-1}), q_e , q_t show quantity of adsorbate adsorbed (in mg g^{-1}) at the equilibrium along with time t (in minute),correspondingly. Slope and intercept of a linear plot of log (q_e-q_t) vs. t were utilized for determining value of rate constants (k_1) and qe, correspondingly

2.6.2. Pseudo-second-order model

This model and equation below may be utilized to explain the adsorption kinetics [33]:

$$\frac{t}{q_e} = \frac{1}{k_2\, q_e^2} + \left(\frac{1}{q_e}\right) \qquad (3)$$

Here, k_2 signifies second-order constant (represented in g mg^{-1} min^{-1}). Values of k_2 and q_e (mg g^{-1}) can be computed utilizing the plot of t/q_e versus t.

2.7. Adsorption Isotherms

2.7.1. Langmuir adsorption isotherm model

The Langmuir isotherm indicates, the adsorbate forms a monolayer and that the adsorption is homogenous. This model's linearised version can be shown as follows [34]:

$$\frac{C_e}{C_q} = \frac{1}{k_l Q_m} + \frac{C_e}{Q_m} \qquad (4)$$

Here kL (L/mg) stands for Langmuir constant while Qm (mg/g) stands for adsorbent's maximal monolayer capacity. Slope and intercept of a plot of Ce versus Ce/qe, correspondingly, may be utilized to predict values of Qm and kL. Viability of the adsorption process at various starting concentrations has been investigated using the dimensionless factor (RL). The subsequent equation was utilized to calculate the RL values:

$$R_L = \frac{1}{1+(k_L C_0)} \qquad (5)$$

Here, C_0 (mg/L) signify initial concentrations of adsorbate species.

2.7.2. Freundlich adsorption isotherm model

Based on the heterogeneous surface of adsorbent's multilayer properties, the Freundlich model explained the connection between equilibrium adsorbate along with adsorbent capacity. This model's logarithmic equation can be written as follows [35]:

$$\ln q_e = \ln k_f + \frac{1}{n}(\ln C_e) \qquad (6)$$

Here Ce (mg/L) stands for equilibrium concentrations of the adsorbates in the solution whereas qe (mg/g) stands quantity of adsorbate adsorbed per unit mass of adsorbent at equilibrium. Adsorption capacity Along with intensity is indicated by the Freundlich constants Kf (L/g) and n, correspondingly. Slope and intercept of a plot of lnqe vs. lnCe have been utilized to calculate the values of the Kf and 1/n.

2.7.3. Temkin adsorption isotherm model

It clarifies both the sorption energy and the indirect interaction among the adsorbent and the adsorbate. The following is an explanation of the Tempkin equation [36]:

$$Q_e = B\ln(k_T) + B\ln(C_e) \qquad (7)$$

Here, kT , B denotes the Tempkin coefficients, determined from the plot of qe against ln Ce.

3. RESULTS AND DISCUSSION

3.1. Characterization

3.3.1. FESEM

It is an important analysis to investigate whether the contaminant got adsorbed or not by the BR and BR/LFNC. It is also used to understand the distribution of molecules, porosity, structure and morphological characteristics. FESEM images of BR and BR/LFNC before and after adsorption of CS are shown in Fig. 1(a-d). BR has uniform and smooth surface. BR/LFNC shows high degree of porosity. Such structure is responsible for enhanced adsorption of CS in BR/LFNC.

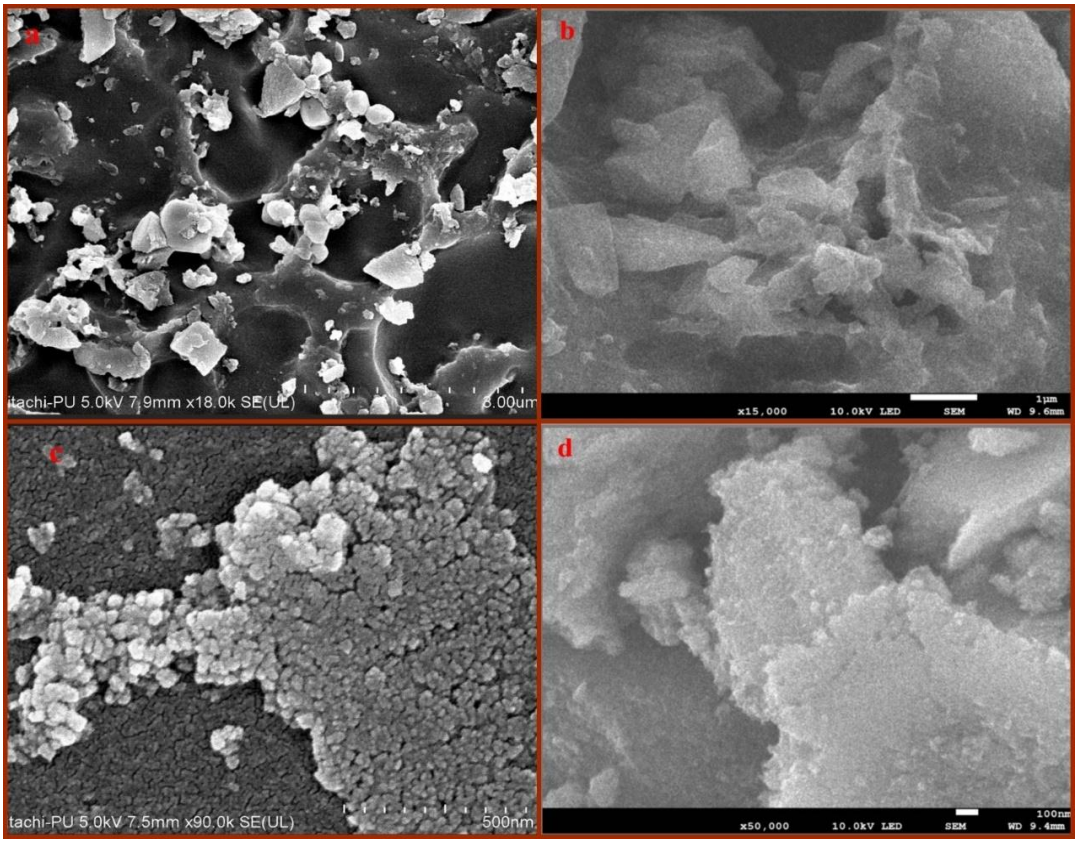

Figure1- FESEM micrographs (a)BR (b) BR loaded CS (c)BR/LFNC (d) BR/LFNC loaded CS

While examining pre-adsorption and post-adsorption images, several deposition patterns can be identified indicated that CS was deposited on the biochar after adsorption tests. Images additionally demonstrate that throughout the adsorption process, pores become covered. Comparable explanations are discussed BR/LFNC adsorbent surfaces. The figures clearly depict the complete adsorption of CS. CS is uniformly adsorbed on the surface of BR and BR/LFNC. The active sites are covered with the CS.

3.1.2. FTIR Study

FTIR had been utilized to detect the different functional groups on t BR and BR/ LFNC's surface. This examination is crucial for comprehending the alterations in the chemical structure of materials found in the sample, including organic, inorganic, and polymeric compounds. Infrared light within the 400–4000 cm^{-1} range is utilised to evaluate the material. The FTIR of BR and BR/LFNC before and after CS adsorption is illustrated in Fig. 2 (a-b) in a clear manner.

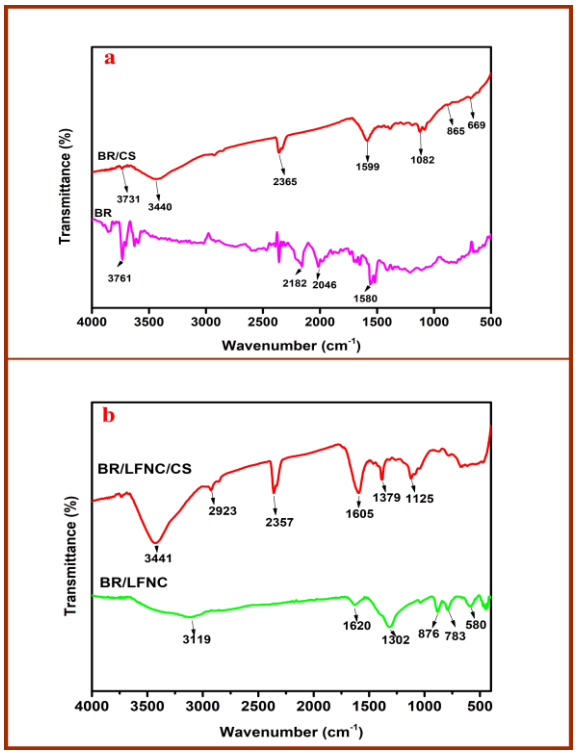

Figure 2- FTIR (a) BR, BR/CS (b) BR/LFNC, BR/LFNC/CS

The BR FTIR spectra show a peak at 1580 cm^{-1} that is representative of highly conjugated C = C or C=C of aromatic ring. Peaks at 2389 cm^{-1} imply either symmetric or asymmetric C-H deformation, whereas at 2182 cm^{-1} stretching vibration of the C=O group is detected. Following CS adsorption, modifications can be detected in the spectra as a different peak in which few variations in intensities may be noted, confirming CS adsorption onto BR. The O-Fe-O bending vibration may be the reason for the peak in the BR/LFNC at 580 cm^{-1}. The peak at 783 cm^{-1} and 876 cm^{-1} emerged because of La-O bending vibration. Big peaks that developed at 1620 cm^{-1} and 3119 cm^{-1}, correspondingly, are caused by H-O-H bending vibration along with -OH stretching vibration [37],[38]. The signal at 1580 cm^{-1} and 3761 cm^{-1} shifts to 1127 cm^{-1} and 2929 cm^{-1}, correspondingly, following the adsorption of CS on BR adsorbent. There is a shift in the signals at 2182 cm^{-1}, 2389 cm^{-1} to 2365 cm^{-1} and 2853 cm^{-1}, correspondingly. Peaks at 580 cm^{-1}, 783 cm^{-1}, 876 cm^{-1}, and 1302 cm^{-1} in BR/LFNC have been displaced to 669 cm^{-1}, 1120 cm^{-1}, 1131 cm^{-1}, 1382 cm^{-1}, correspondingly. Peak, which was at 1620 cm^{-1}, is now at 1595 cm^{-1}. The interaction of CS with BR and BR/LFNC surfaces is suggested for the shifting of the adsorption peaks.

3.2. Optimization of different parameters

3.2.1. Effect of initial concentration of adsorbate

Investigations on differences in the starting concentration of CS, which ranged from 20 ppm to 60 ppm, were conducted in phases. At 20 ppm, the greatest elimination percentage was noted. Fig. 3(a) clearly shows the percentage of adsorption decreases from 66% to 52% and from 78% to 60%, by using BR and BR/LFNC respectively. This is because the active sites' surface area was saturated, which led to a drop in the removal percentage. In comparison to its BR/LFNC, BR displayed a lower removal %. This can be attributed to BR having fewer active sites than BR/LFNC [39].

3.2.2. Effect of pH

With 0.2 g of biochar, the effects of pH on a 20 ppm CP solution were studied. Here, 0.1M concentrations of NaOH along with HCl had been utilized to change solution's pH between 2 and 10. It is clear from Fig. 3(b) at pH 4.0, the maximum amount of CS 71% and 80% was removed from BR and BR/LFNC respectively. Following that, the adsorption decreases. Since the adsorbent's surface has been charged positively and CS is present in anionic form, there is a substantial electrostatic attraction between them at pH values below 4.5, which is the adsorbent's point of zero charge (BR/LFNC). Adsorbent's surface acquires negatively charged above this pH, and at higher pH values, there is interionic repulsive action with the OH ion [40]-[42].

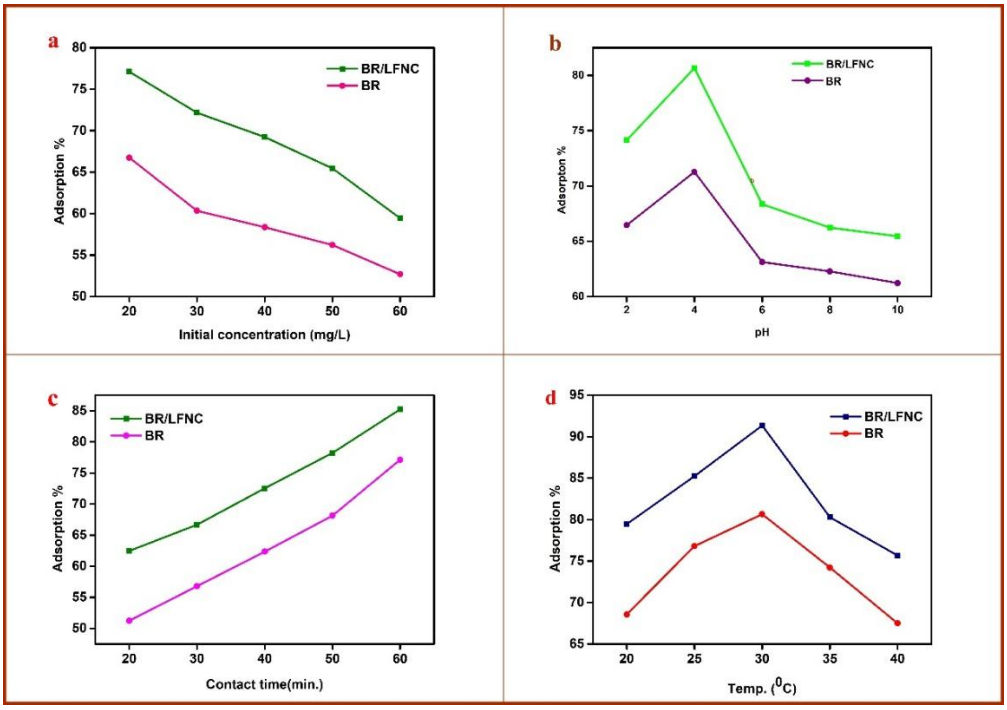

Figure 3- Optimised parameters (a) effect of initial adsorbate concentration (b) effect of pH (c) effect of agitation time (d) effect of Temperature

3.3.3. Effect of contact time

CS solution's maximal adsorption capacity had been shown to rise for up to 60 minutes on 0.2 g biochar in 20 ppm synthetic CS solution Fig. 3(c). This suggests that maximum adsorption can be attained in 60 minutes after which the biochar reaches its saturation point. This is due to its improved surface covering. It was discovered that, up to 77 % of the CS on BR was eliminated. It was concluded that 60 minute was the maximum elimination time. Similarly, 85 % of CS was adsorbed by BR/LFNC in 60 minutes [43].

3.3.4. Effect of temperature

Temperature had been adjusted for a 20 ppm CS solution with 0.2 g of biochar and shaken for 60 minutes, between 20 to 40 °C (every 5 °C). Fig. 3(d) demonstrates that maximum adsorption was achieved at 30 ^{0}C i.e. 80 % and 91 % by employing BR and BR/LFNC adsorbents respectively. The activation and widening of the porous structure of the adsorbent surface were the cause of the enhanced adsorption [44,45].

3.4. Isotherm and kinetic study

Furthermore, the Langmuir, Freundlich, alongwith Tempkin models are 3 renowned isotherm models, that have been employed to examine the adsorption nature as well as mechanism of adsorbents (BR, BR/LFNC). Fig. 4 (a-c) displays the linear fitting plots for the experimental data following their fitting.

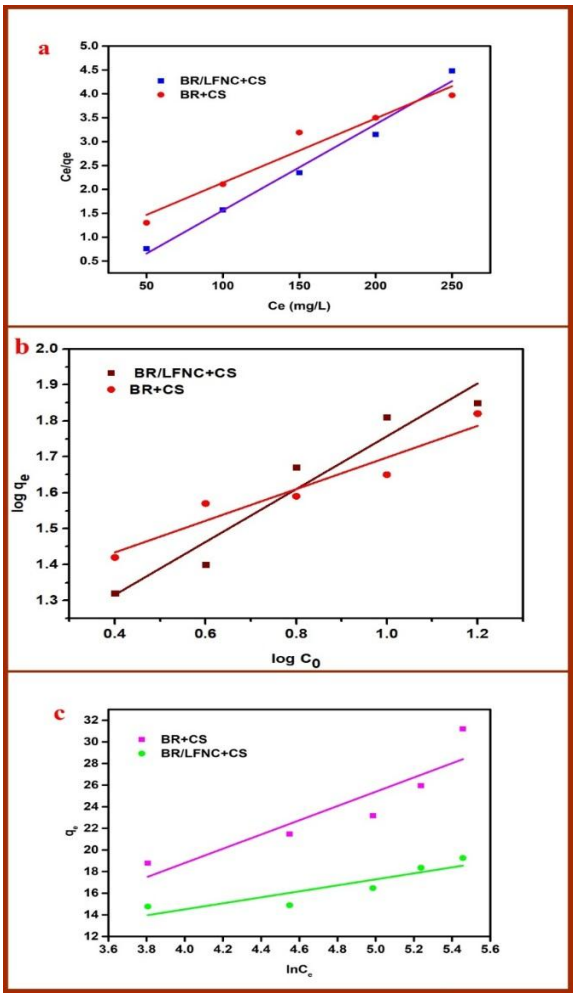

Figure 4 - Isotherm model (a) Langmuir (b) Freundlich (c) Tempkin

As per the Langmuir model, the Freundlich, Tempkin isotherm does not offer a linear match. Isotherm model's highest correlation coefficient (R^2) has been given precedence. The model's utility is further demonstrated by the lower regression coefficient (R^2) value of Freundlich (R^2= 0.93), Tempkin model (R^2= 0.76). Langmuir model was shown as appropriate for understanding CS's adsorption behaviour onto an adsorbent due to its higher R^2 value (0.94), (0.98) for BR and BR/LFNC correspondingly. The Langmuir model provided an explanation of the adsorption mechanism, demonstrated that CS molecules sorb onto adsorbent molecules in a monolayer and advantageously.

Kinetic parameters for the CS's adsorption from adsorption from aqueous phase had been thoroughly examined. To analyse the kinetic experimental data, the pseudo-first-order along with pseudo-second-order model had been used as Fig. 5(a-b) illustrated. kinetics model's applicability was evaluated utilizing a variety of fitting graphs. The kinetics of CS adsorption onto BR and BR/LFNC were sufficiently elucidated through a pseudo-second-order with higher regression coefficient values (R^2 = 0.98). As a result, the chemical mechanism mostly governed the adsorption process.

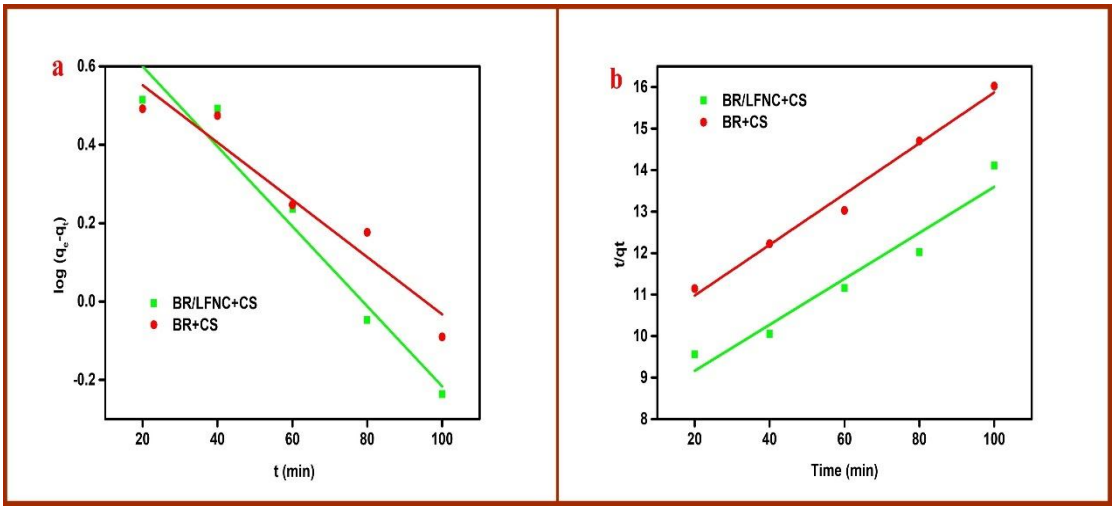

Figure 5- Kinetic model (a) pseudo first order model (b) pseudo second order model

3.5. Recyclability and stability

Renewable and reusability of adsorbent was shown to be important factor. As seen in Fig.6 BR and BR/LFNC were examined for the reuse test. Despite this, there was no discernible decrease in activity after five cycles, indicating the stability of the adsorbent. In order to assess the adsorbent's durability, reusability tests were carried out for a maximum of five consecutive cycles. In order to remove the pesticide molecules that had been adsorbed, the adsorbent was repeatedly cleaned with distilled water for each cycle. It was then dried at 75 °C for future usage. After five cycles of usage adsorption capacity of BR was 78.34 % and that of BR/LFNC was 93.12%.

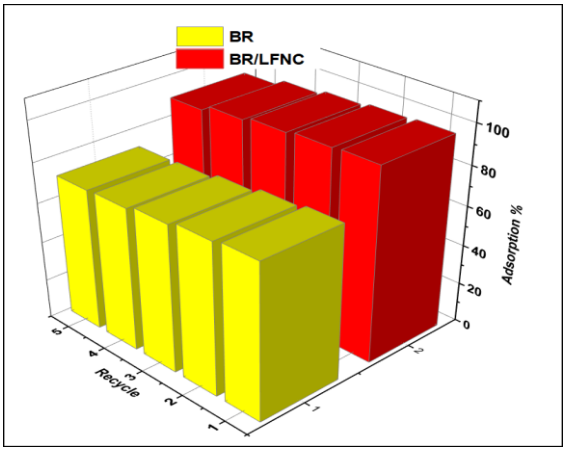

Figure 6- Recycle study of chlorpyrifos adsorption

CONCLUSION

The current study used Syzygium cumini biochar (BR) and its lanthanum ferrite nanocomposite (BR/LFNC) to study CS's adsorption from the aqueous phase. Chemical compositions as well as surface features of BR, BR/LFNC were investigated using FTIR and FESEM equipment techniques. The

solution's pH had a substantial impact on the adsorption behaviour of adsorbate molecules. At pH 4.0, the greatest amount of CS adsorption was observed. Equilibrium sorption of the adsorbates onto BR, BR/LFNC was accurately described by Langmuir model with higher R^2 values of 0.94 and 0.98. Chlorpyrifos (CS) has been endothermically and spontaneously extracted from the aqueous phase, according to the thermodynamic analysis. However, even after five cycles, desorption tests showed that (CS) might be effectively eliminated from adsorbent surfaces as well as possess a greater adsorption uptake (%). It has been discovered that the BR/LFNC nano-composite is superior in terms of increased stability, adsorption capacity and reuse. Consequently, the current research reveals a unique adsorbent that is both environmentally safe and promising for the removal of chlorpyrifos (CS) from water systems. Additionally, the present research will encourage the lanthanum-based nanocomposites creation from several agricultural waste, that have larger surface area and can be used for transdisciplinary environmental remediation.

ACKNOWLEDGEMENT

Authors wish to express their gratitude to Indian Institute of Technology (IIT), Mandi, and Punjab University (PU), India for providing the necessary instrumental facility to carry outpresent research work.

Conflict of interest

The authors declare that they have no known competing financial interest or personal relationships that could have appeared to influence the research work.

Funding Source

There was no funding.

Ethical approval

This research did not involve human participants, animal subjects, or any material that requires ethical approval.

Informed Consent Statement

This study did not involve human participants, and therefore, informed consent was not required.

Credit authorship contribution statement Anita Kumari: Investigation, Formal analysis, Methodology, conceptualization. Arush Sharma: Writing – review & editing, Writing – original draft, Validation, Software, Data curation. Anita Rani: Conceptualization.

REFERENCES

[1] Pathania D., Dhar S., Sharma A., Srivastava A.K. Decolourization of noxious safranin-T from waste water using Mangifera indica as precursor. *Environ. Sustain*. 2021;4:355-64.

[2] Iftekhar S., Ramasamy D.L., Srivastava V., Asif M.B., Sillanpää M. Understanding the factors affecting the adsorption of Lanthanum using different adsorbents: a critical review. *Chemosphere.* 2018;204:413-30.

[3] Alizadeh R., Rafati L., Ebrahimi A.A., Sedighi Khavidak S. Chlorpyrifos bioremediation in the environment: A review article. *J.Environ. Health Sustain. Dev*. 2018;3(3):606-15.

[4] Peng W., Lam S.S., Sonne C. Support Austria's glyphosate ban. *Science*. 2020 ;367(6475):257-8.

[5] Pathania D., Sharma A. Microwave induced graft copolymerization of binary monomers onto luffa cylindrica fiber: removal of congo red. *Procedia Eng*. 2017;200:408-15.

[6] Devipriya S., Yesodharan S. Photocatalytic degradation of pesticide contaminants in water. *Sol. Energy Mater. Sol. Cells.* 2005;86(3):309-48.

[7] Topkaya E., Konyar M., Yatmaz H.C., Öztürk K. Pure ZnO and composite ZnO/TiO2 catalyst plates: a comparative study for the degradation of azo dye, pesticide and antibiotic in aqueous solutions. *J. Colloid Interface Sci.* 2014;430:6-11.

[8] Racke K.D. Environmental fate of chlorpyrifos. Reviews of Environmental Contamination and Toxicology: Continuation of Residue Reviews. 1993:1-50.

[9] Moradeeya P.G., Kumar M.A., Thorat R.B., Rathod M., Khambhaty Y., Basha S. Nanocellulose for biosorption of chlorpyrifos from water: chemometric optimization, kinetics and equilibrium. *Cellulose*. 2017;24:1319-32.

[10] Liu H., Chen J., Wu N., Xu X., Qi Y., Jiang L., Wang X., Wang Z. Oxidative degradation of chlorpyrifos using ferrate (VI): Kinetics and reaction mechanism. *Ecotoxicol. Environmental safety.*2019;170:259-66.

[11] Sivagami K., Vikraman B., Krishna RR., Swaminathan T. Chlorpyrifos and Endosulfan degradation studies in an annular slurry photo reactor. *Ecotoxicology and environ. Saf* .2016;134:327-31.

[12] Qurie M., Khamis M., Ayyad I., Scrano L., Lelario F., Bufo SA., Mecca G., Karaman R. Removal of chlorpyrifos using micelle–clay complex and advanced treatment technology. *Desalin Water Treat*. 2016;57(33):15687-96.

[13] Gennari M., Messina C., Abbate C., Baglieri A., Boursier C. Solubility and adsorption behaviors of chlorpyriphos-methyl in the presence of surfactants. *J. Environ. Sci Health B*. 2009;44(3):235-40.

[14] Munoz A.R., Trevisan M., Capri E. Sorption and photodegradation of chlorpyrifos on riparian and aquatic macrophytes. *J. Environ. Sci Health B*. 2008 ;44(1):7-12.

[15] Vigneshwaran S., Preethi J., Meenakshi S. Removal of chlorpyrifos, an insecticide using metal free heterogeneous graphitic carbon nitride (g-C3N4) incorporated chitosan as catalyst: photocatalytic and adsorption studies. *Int. J. Biol Macromol*. 2019;132:289-99.

[16] Dawood S., Sen T.K., Phan C. Synthesis and characterization of slow pyrolysis pine cone bio-char in the removal of organic and inorganic pollutants from aqueous solution by adsorption: kinetic, equilibrium, mechanism and thermodynamic. *Bioresour. Technol*. 2017 ;246:76-81.

[17] Zheng H., Zhang Q., Liu G., Luo X., Li F., Zhang Y., Wang Z. Characteristics and mechanisms of chlorpyrifos and chlorpyrifos-methyl adsorption onto biochars: Influence of deashing and low molecular weight organic acid (LMWOA) aging and co-existence. *Sci. Total Environ.* 2019;657:953-62.

[18] Taha SM., Amer M.E., Elmarsafy A.E., Elkady M.Y. Adsorption of 15 different pesticides on untreated and phosphoric acid treated biochar and charcoal from water. *J. Environ. Chem. Eng.* 2014;2(4):2013-25.

[19] Wang Y., Hu Y'., Zhao X., Wang S., Xing G. Comparisons of biochar properties from wood material and crop residues at different temperatures and residence times. *Energy Fuels*. 2013 ;27(10):5890-9.

[20] Soto ML., Moure A., Domínguez H., Parajó J.C. Recovery, concentration and purification of phenolic compounds by adsorption: A review. *J. Food Engin*. 2011;105(1):1-27.

[21] Allen SJ, Gan Q, Matthews R, Johnson PA. Comparison of optimised isotherm models for basic dye adsorption by kudzu. *Bioresour Technol*. 2003;88(2):143-52.

[22] Zhou Y, Zhang L, Cheng Z. Removal of organic pollutants from aqueous solution using agricultural wastes: a review. *J. Mol. Liq*. 2015;212:739-62.

[23] Qi F., Yan Y., Lamb D., Naidu R., Bolan N.S., Liu Y., Ok YS., Donne S.W., Semple K.T. Thermal stability of biochar and its effects on cadmium sorption capacity. *Bioresour Technol* . 2017;246:48-56.

[24] Varjani S, Kumar G, Rene ER. Developments in biochar application for pesticide remediation: current knowledge and future research directions. *J.Environ.Manag.*2019 ;232:505-13.

[25] Eduah JO, Nartey EK, Abekoe MK, Henriksen SW, Andersen MN. Mechanism of orthophosphate (PO4-P) adsorption onto different biochars. *Environ. Technol. Innov.* 2020 ;17:100572.

[26] Ao H., Cao W., Hong Y., Wu J., Wei L. Adsorption of sulfate ion from water by zirconium oxide-modified biochar derived from pomelo peel. *Sci Total Environ.* 2020;708:135092.

[27] Silos-Llamas A.K., Durán-Jiménez G., Hernández-Montoya V., Montes-Morán M.A., Rangel-Vázquez N.A. Understanding the adsorption of heavy metals on oxygen-rich biochars by using molecular simulation. *J. Mol. Liq.* 2020 ;298:112069.

[28] Yang X., Zhang S., Liu L., Ju M. Study on the long-term effects of DOM on the adsorption of BPS by biochar. *Chemosphere.* 2020 ;242:125165.

[29] Zhao J., Shen X.J., Domene X., Alcañiz J.M., Liao X., Palet C. Comparison of biochars derived from different types of feedstock and their potential for heavy metal removal in multiple-metal solutions. *Sci. Rep*. 2019;9(1):9869.

[30] Chakraborty I., Das S., Dubey B.K., Ghangrekar M.M. Novel low cost proton exchange membrane made from sulphonated biochar for application in microbial fuel cells. *Mater. Chem. Phys*.2020 ;239:122025.

[31] Feng Y., Li D., Liu J., He W. Carbon-based materials in microbial fuel cells. In Microbial electrochemical technology 2019 Jan 1 (pp. 49-74). Elsevier.

[32] Guo Q., Ma Q., Xue Z., Gao X., Chen H. Studies on the binding characteristics of three polysaccharides with different molecular

weight and flavonoids from corn silk (Maydis stigma). *Carbohydr. Polym*. 2018;198:581-8.

[33] Tolić K., Mutavdžić Pavlović D., Stankir N., Runje M. Biosorbents from tomato, tangerine, and maple leaves for the removal of ciprofloxacin from aqueous media. *Water Air Soil Pollut* .2021;232(5):218.

[34] Yan L., Dong F.X., Li Y., Guo P.R., Kong L.J., Chu W., Diao ZH. Synchronous removal of Cr (VI) and phosphates by a novel crayfish shell biochar-Fe composite from aqueous solution: Reactivity and mechanism. *J. Environ. Chem. Eng*. 2022 ;10(2):107396.

[35] Afzal M.Z., Sun X.F., Liu .J, Song C., Wang S.G., Javed A. Enhancement of ciprofloxacin sorption on chitosan/biochar hydrogel beads. *Sci Total Environ*. 2018 ;639:560-9..

[36] Sharma A., Siddiqi Z.M., Pathania D. Adsorption of polyaromatic pollutants from water system using carbon/ZnFe2O4 nanocomposite: equilibrium, kinetic and thermodynamic mechanism. . *J. Mol. Liq*. 2017;240:361-71.

[37] Kumari A., Kumar A., Pathania D., Thakur M., Sharma A. Biochar derived from Syzygium cumini seed embedded nanohybrid structure for eco-friendly remediation of Cr (VI) and As (III) ions: Adsorption and modeling analysis. *SCENV*. 2025 ;9:100189.

[38] Ottman N., Ruokolainen L., Suomalainen A., Sinkko H., Karisola P., Lehtimäki J., Lehto M., Hanski .I, Alenius H., Fyhrquist N. Soil exposure modifies the gut microbiota and supports immune tolerance in a mouse model. . *J. Allergy Clin. Immunol*. 2019;143(3):1198-206.

[39] Abukhadra M.R., Ibrahim S.M., Khim J.S., Allam A.A., Ajarem J.S., Maodaa S.N. Enhanced decontamination of pefloxacin and chlorpyrifos as organic pollutants using chitosan/diatomite composite as a multifunctional adsorbent; equilibrium studies *J. Sol-Gel Science and Technol*. 2021;99(3):650-62.

[40] ul Haq A, Saeed M, Usman M, Naqvi SA, Bokhari TH, Maqbool T, Ghaus H, Tahir T, Khalid H. Sorption of chlorpyrifos onto zinc oxide nanoparticles impregnated Pea peels (Pisum sativum L): Equilibrium, kinetic and thermodynamic studies. *Environ. Technol. Innov.* 2020 ;17:100516.

[41] Hamadeen HM., Elkhatib E.A. Nanostructured modified biochar for effective elimination of chlorpyrifos from wastewater: Enhancement, mechanisms and performance. *J.Water Process Eng*. 2022;47:102703..

[42] Wang P., Yin Y., Guo Y., Wang C. Removal of chlorpyrifos from waste water by wheat straw-derived biochar synthesized through oxygen-limited method. *RSC advances*. 2015;5(89):72572-8.

[43] Vigneshwaran S., Preethi J., Meenakshi S. Removal of chlorpyrifos, an insecticide using metal free heterogeneous graphitic carbon nitride (g-C3N4) incorporated chitosan as catalyst: Photocatalytic and adsorption studies. . *Int. J. Biol. Macromol*. 2019 ;132:289-99.

[44] Jacob M.M., Ponnuchamy M., Kapoor A., Sivaraman P. Bagasse based biochar for the adsorptive removal of chlorpyrifos from contaminated water. *J. Environ. Chem. Eng*. 2020;8(4):103904..

[45] Alsherbeny S., Jamil T.S., El-Sawi S.A., Eissa F.I. Low-cost corn cob biochar for pesticides removal from water. *Egypt. J. Chem*. 2022;65(2):639-50.